Journal of Vibration Engineering & Technologies (2023) 11:1867–1888
https://doi.org/10.1007/s42417-022-00676-9

ORIGINAL PAPER

Vibration of CFFF Functionally Graded Plates with an Attached Point Mass at an Arbitrary Point in Thermal Environment

Bahar Uymaz[1]

Received: 11 May 2022 / Revised: 8 August 2022 / Accepted: 11 August 2022 / Published online: 18 September 2022

Abstract
Purpose In many cases, working on models such as carrying a point attached mass or distributed attached mass provides a more realistic depiction of the problem. The main reason for the vibration studies of the structural elements with coupled mass, which constitute the main purpose of this study, is to see the changes in the resonance frequency due to the attached mass and to reduce the resonance frequency to a desired value. Although the vibration problems of mass-loaded rectangular plates are a very common problem in engineering applications, no study on functionally graded plates has been found in the literature. In this study, the effect of the variation of temperature-dependent material properties along the thickness according to a simple power law on the vibration behavior of point mass carrying functionally graded plates is investigated for the cantilever (CFFF) boundary condition. Numerical studies are performed for different mass ratio (M), different location of point mass on the plate region and throughout the x axis, volume fractions with p and side-to-side ratio (a/b) at nonlinear temperature distribution.
Methods In this study, effect of the mass and temperature on free vibration of the functionally graded plate carrying a point mass at an arbitrary position is analysed with three-dimensional Ritz solution. Material properties of considered functionally graded plate are assumed to be temperature dependent and reinforcement in thickness direction according to a power law distribution and effective material properties are estimated using Mori-Tanaka homogenization method.
Results Free vibration frequencies decrease with increasing p index and increasing temperature difference. The frequencies obtained in the case of with point mass are always smaller than the frequency values obtained in the case of without point mass. When the point mass is located on a nodal line, the mass does not move during these and so frequency remains constant as independent of the presence of mass. If the mass is located on the nodal lines, at these frequencies it will resonate at the natural frequency of the unperturbed plate.
Conclusion The study shows that the effect of the presence of added mass, mass size and location on structures may not be negligible.

Keywords Free vibration · Attached point mass · Nonlinear temperature distribution · Functionally graded plate · Mori–Tanaka homogenization scheme · Ritz method

Introduction

Functionally graded materials (FGMs) are designed for the first time in 1984 by Japanese scientists [1, 2] as high temperature resistant materials, especially for structures such as aircraft, spacecraft and other engineering structures. FGMs are high-tech materials in which the desired thermal and mechanical properties can be produced by continuously changing the material properties in a thickness and/or in-plane direction. These advanced properties of FGMs have allowed them to be considered as materials for structures modeled as structural elements such as plates, beams, and shells. Free vibration analysis of structural elements with FGM-designed plate geometry has always attracted the attention of researchers.

A simple yet effective first order shear deformation plate theory integrated with meshfree moving Kriging method has been developed by Vu et al. [3] for the analysis of

✉ Bahar Uymaz
buymaz@nku.edu.tr

[1] Engineering Faculty, Department of Mechanical Engineering, Tekirdağ Namık Kemal University, Çorlu, 59860 Tekirdağ, Turkey

free vibration and static deflection of functionally graded ceramic–metal plates. Zhao et al. [4] presented a free vibration analysis of functionally graded rectangular and skew plates with used the element-free kp-Ritz method based on first order shear deformation theory under clamped, simply supported and cantilever boundary conditions. The free vibration and static analysis of square and rectangular functionally graded plates was presented, which is based on the higher order shear deformation theory with a new finite element model by Talha ve Singh [5]. In the study the systems of algebraic equations were derived using variational approach for the free vibration and static problem. Nguyen [6] proposed a higher order hyperbolic shear deformation plate model for bending, buckling and vibration analysis of functionally graded plates. Ferreira et al. [7] used the asymmetric collocation method with multiquadrics basis functions, and the FSDT and the TSDT to obtained natural frequencies of square functionally graded plates. Matsunaga [8] presented a 2-dimensional high-order theory in which the full effects of shear deformations, thickness changes and rotational inertia are taken into account to analyze the natural frequencies and buckling stresses of functionally graded plates. Exact free vibration analysis of moderately thick and thick functionally graded plates using two-dimensional higher order kinematic theories which considered both shear and normal deformation effects is investigated by used Levy method by Dozio [9].

A unified and accurate solution method has been developed by Jin et al. [10] to deal with the free vibration analysis of arbitrarily thick functionally graded plate with general boundary based on the linear, small-strain 3D elasticity theory. Vel and Batra [11] presented a three-dimensional exact solution for the vibration of simply supported rectangular thick functionally graded plates. In the study the effective material properties at a point were estimated from the local volume fractions and the material properties of the phases either by the Mori–Tanaka [12, 13] or the self-consistent [14] scheme. Uymaz and Aydoğdu [15] carried out the Ritz method with Chebyshev polynomials for the free vibration analysis of functionally graded plates based on three-dimensional elasticity.

Free vibration analysis of simply supported functionally graded plates is numerically studied using QUAD-8 shear flexible element with and without thermal environment based on first order shear deformation theory by Natarajan et al. [16]. The effective material properties are estimated using Mori–Tanaka homogenization method.

A theoretical method was developed to investigate vibration characteristics of initially stressed functionally graded rectangular platesmade up of metal and ceramic in thermal environment by Kim [17]. Free vibration of functionally graded material rectangular plates with simply supported and clamped edges in the thermal environment was studied based on the three-dimensional linear theory of elasticity by Li et al. [18].

However, in many cases, working on models such as carrying a point attached mass or distributed attached mass provides a more realistic depiction of the problem. The main reason for the vibration studies of the structural elements with coupled mass, which constitute the main purpose of this study, is to see the changes in the resonance frequency due to the attached mass and to reduce the resonance frequency to a desired value.

Gürgöze et al. [19] investigated free vibration of a cantilever euler–bernoulli beam carrying a tip mass with in-span support using the Dunkerley's procedure. Cha and Wong [20] presented a method to analyze free vibration of combined dynamical system which consist of a uniform cantilever Euler–Bernoulli beam carrying an undamped oscillator system using the Lagrange multiplier method and the Green function method.

The free vibration analysis of an isotropic simply supported plate carrying a uniformly distributed mass was investigated by Kopmaz and Telli [21]. The analysis was carried out using the Galerkin procedure, the equation of motion was reduced to a set of ordinary differential equations based on clasical plate theory. This polynomial equation was solved numerically. Wong [22] performed Ritz method based on classical plate theory for solved the free bending vibration of a simply supported rectangular plate carrying distributed mass. Free vibration of isotropic plate carrying distributed spring mass using Ritz-Galerkin method with Chebyshev polynomial series based on classical plate theory by Zhou and Ji [23]. Alibeigloo et al. [24] investigated the free vibration of simply supported angle-ply laminated plates carrying distributed attach mass using the Hamilton's Principle by means of a double Fourier series based on a third-order shear deformation theory.

Chiba and Sugimoto [25] analyzed free vibration of a cantilever plate carrying spring-mass system using Rayleigh–Ritz method based on classical plate theory. Yu [26] presented analytical solutions for free and forced vibrations of cantilever plates carrying single attached mass using Gorman's method of superposition and the modal summaton method. Ciancio et al. [27] presented the vibration problem for a cantilever anisotropic plate carrying a concentrated mass on of center using Ritz method with beam functions based on the classical plate theory. Vibration of symmetrically laminated composite plate carrying an attached mass on of center using Ritz method with simple polynomials based on the classical plate theory is analyzed by Aydoğdu and Filiz [28].

An experimental study on vibration response of an elastically point-supported isotropic plate carrying an attached point mass was presented by Watkins et al. [29]. These results are compared to frequencies and to modes shapes

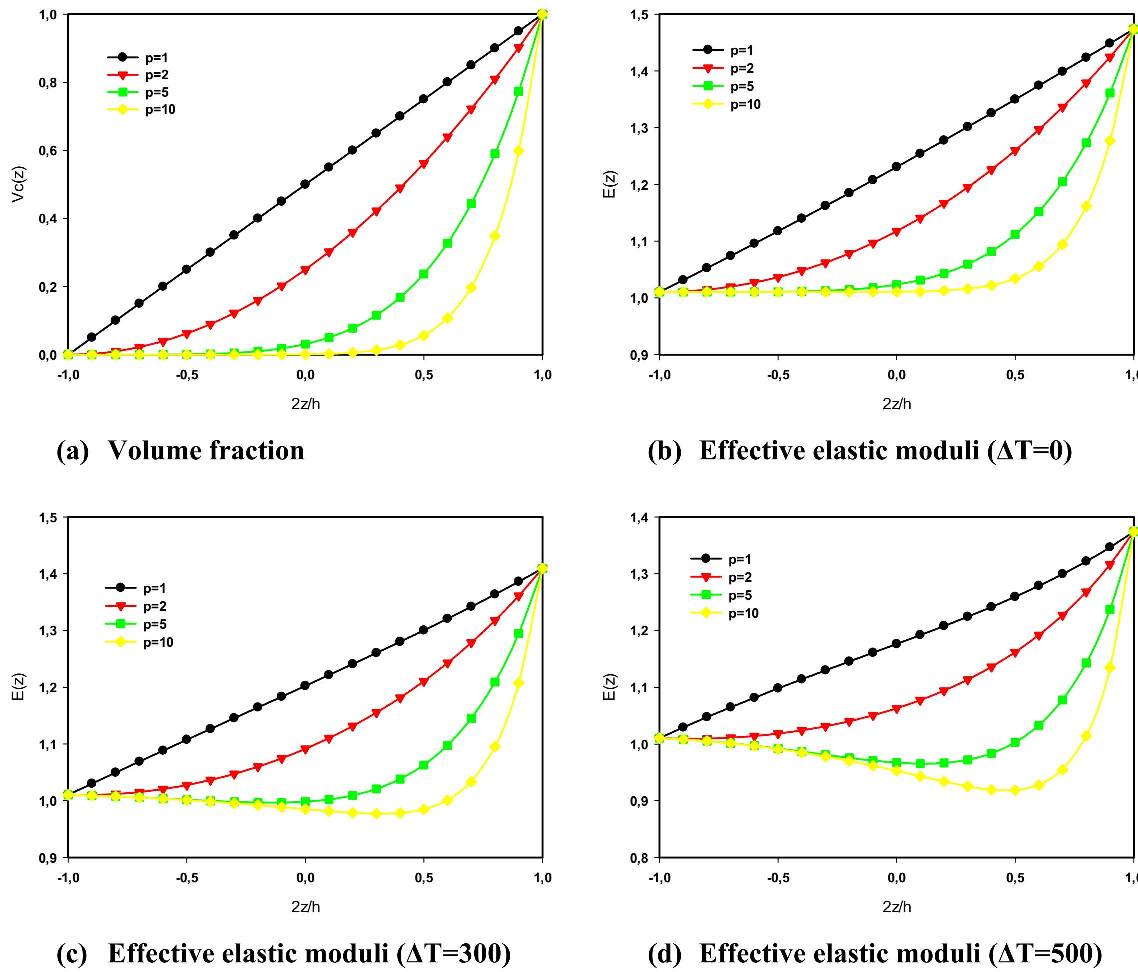

Fig. 1 Volume fraction through the nondimensional thickness co-ordinate, and effective elastic moduli estimated by the Mori–Tanaka scheme with nonlinear temperature distribution

determined from the Rayleigh–Ritz method and a finite element analysis using COMSOL. Ritz method is performed with Orthogonal polynomials as admissible functions, and finite element analysis is based on Mindlin plate theory, adjusted for negligible transverse shear effects.

Khalili et al. [30] studied free vibration of simply supported laminated composite cylindrical shells with uniformly distributed attached mass using Galerkin method based on higher order shell theory including stiffness effect.

Free vibration of clamped thin elliptical plates carrying a concentrated mass at an arbitrary position using Ritz method by polynomial expressions as admissible functions was researched by Maiz et al. [31].

Although the vibration problems of mass-loaded rectangular plates are a very common problem in engineering applications, no study on functionally graded plates has been found in the literature. In this study, the effect of the variation of temperature-dependent material properties along the thickness according to a simple power law on the vibration behavior of point mass carrying functionally graded plates is investigated for the cantilever (CFFF) boundary condition. Numerical studies are performed for different mass ratio (M), different location of point mass on the plate region and throughout the x axis, volume fractions with p and side-to-side ratio (a/b) at nonlinear temperature distribution.

Problem Formulation

In this study, effect of the mass and temperature on free vibration of the functionally graded plate carrying a point mass at an arbitrary position is analyzed with three-dimensional Ritz solution. Material properties of considered functionally graded plate are assumed to be temperature dependent and reinforcement in thickness direction according to a power law distribution and effective material properties are estimated using Mori–Tanaka homogenization method.

Effective Material Properties of Functionally Graded Plates

The lower surface of the considered plate consists of the metal phase and the upper surface of the ceramic phase, and the ceramic phase varies according to a power law distribution in the thickness direction, and it is also assumed that material properties of both phases are temperature dependent. The sum of volume fraction of ceramic and metal phases is

$$V_{\mathrm{c}} + V_{\mathrm{m}} = 1, \tag{1}$$

and the ceramic volume fraction distribution in the thickness direction is as follows.

$$V_{\mathrm{c}}(z) = \left(\frac{z}{h} + \frac{1}{2}\right)^{p}. \tag{2}$$

Here, the p value, which is called the volume ratio exponent, takes values in the range of $0 \leq p \leq \infty$ and shows the amount of ceramic volume ratio. As can be seen in Fig. 1(a), when the p value is 0, the material is full ceramic, when the p value is 1, the variation of the ceramic material in the thickness direction is linear, when $p > 1$ the amount of ceramic increases and when $p < 1$, the amount of ceramic increases with a decrease. In general, an increase in the p value means a decrease in the ceramic volume ratio.

The Mori–Tanaka scheme assumes that isotropic particles are randomly dispersed within the isotropic matrix material. In this study, the matrix phase is metal and the particle phase is ceramic. The effective material properties Young modulus (E), poisson ratio (υ) and thermal coefficients (α) of functionally graded plate which defined according to the Mori–Tanaka homogenization scheme are given as follows,

$$E = \frac{9KG}{3K + G}, \tag{3}$$

$$v = \frac{3K - 2G}{2(3K + G)}, \tag{4}$$

$$\frac{\alpha - \alpha_{\mathrm{m}}}{\alpha_{\mathrm{c}} - \alpha_{\mathrm{m}}} = \frac{\left(\frac{1}{\kappa} - \frac{1}{\kappa_{\mathrm{m}}}\right)}{\left(\frac{1}{\kappa_{\mathrm{c}}} - \frac{1}{\kappa_{\mathrm{m}}}\right)}. \tag{5}$$

In here the effective Bulk modulus K, the effective shear modulus G and the effective heat conductivity κ are defined as follows,

$$\frac{\kappa - \kappa_{\mathrm{m}}}{\kappa_{\mathrm{c}} - \kappa_{\mathrm{m}}} = \frac{V_{\mathrm{c}}}{1 + \left(1 - V_{\mathrm{c}}\right)\frac{\left(\kappa_{\mathrm{c}} - \kappa_{\mathrm{m}}\right)}{2\kappa_{\mathrm{m}}}}, \tag{6}$$

$$\frac{K - K_{\mathrm{m}}}{K_{c} - K_{\mathrm{m}}} = \frac{V_{\mathrm{c}}}{1 + \left(1 - V_{c}\right)\frac{3\left(K_{\mathrm{c}} - K_{m}\right)}{3K_{\mathrm{m}} + 4G_{\mathrm{m}}}}, \tag{7}$$

$$\frac{G - G_{\mathrm{m}}}{G_{\mathrm{c}} - G_{\mathrm{m}}} = \frac{V_{\mathrm{c}}}{1 + \left(1 - V_{\mathrm{c}}\right)\frac{\left(G_{\mathrm{c}} - G_{\mathrm{m}}\right)}{G_{\mathrm{m}} + \mathrm{f}_{1}}}, \tag{8}$$

where

$$f_{1} = \frac{G_{\mathrm{m}}\left(9K_{\mathrm{m}} + 8G_{\mathrm{m}}\right)}{6\left(K_{\mathrm{m}} + 2G_{\mathrm{m}}\right)}, \tag{9}$$

The effective mass density (ρ) of functionally graded plate which defined according to the rule of mixtures is given as follow,

$$\rho = V_{\mathrm{c}}\left(\rho_{\mathrm{c}} - \rho_{\mathrm{m}}\right) + \rho_{m}. \tag{10}$$

The sub-indices c and m used in the equations given above represent ceramic and metal materials, respectively. Variation of the nondimensional effective elastic moduli throughout the nondimensional thickness co-ordinate estimated by the Mori–Tanaka scheme are given in Fig. 1(b)–(d) for various temperature in nonlinear thermal environment.

Stress–Strain Relations Based on Three-Dimensional Elasticity

The considered thin functionally graded plate in this paper is in the form of rectangular with length a, width b and thickness h. The origin of the co-ordinate system (x,y,z) is placed at the geometric center of the plate and the axes are parallel to the edges of the plate and the corresponding displacement components u, v and w along the x, y and z directions, respectively. For free vibration problem based on three-dimensional elasticity theory the displacement field is as follows,

$$\begin{aligned} u(x, y, z;t) &= U(x, y, z)e^{i\omega t}; v(x, y, z;t) \\ &= V(x, y, z)e^{i\omega t}; w(x, y, z;t) = W(x, y, z)e^{i\omega t}, \end{aligned} \tag{11}$$

where ω corresponds the natural frequency of the plate and $i = \sqrt{-1}$. The strain components $\varepsilon_{\mathrm{ij}}$ (i,j = x,y,z) for small deformations are given as,

$$\varepsilon_{\mathrm{x}} = u_{,\mathrm{x}}; \varepsilon_{\mathrm{y}} = v_{,\mathrm{y}}; \varepsilon_{\mathrm{z}} = w_{,\mathrm{z}}, \tag{12}$$

$$\gamma_{\mathrm{yz}} = v_{,\mathrm{z}} + w_{,\mathrm{y}};\ \gamma_{xz} = u_{,\mathrm{z}} + w_{,\mathrm{x}}; \gamma_{\mathrm{xy}} = u_{,\mathrm{y}} + v_{,\mathrm{x}}, \tag{13}$$

where$_{,(x,y,z)} = \left(\frac{\partial}{\partial x}, \frac{\partial}{\partial y}, \frac{\partial}{\partial z}\right)$. The stress–strain relations for a linear elastic isotropic material are given by the generalized Hooke's law as follows,

$$\sigma_x = C_{11}\varepsilon_x + C_{12}\varepsilon_y + C_{12}\varepsilon_z, \tag{14}$$

$$\sigma_y = C_{12}\varepsilon_x + C_{11}\varepsilon_y + C_{12}\varepsilon_z, \tag{15}$$

$$\sigma_z = C_{12}\varepsilon_x + C_{12}\varepsilon_y + C_{11}\varepsilon_z, \tag{16}$$

$$\tau_{yz} = C_{66}\gamma_{yz}, \tag{17}$$

$$\tau_{xz} = C_{66}\gamma_{xz}, \tag{18}$$

$$\tau_{xy} = C_{66}\gamma_{xy}, \tag{19}$$

where $[C]$ is stiffness matrix and its components are defined as follows,

$$C_{11}(z,T)=\frac{E(z,T)(1-\nu(z,T))}{(1+\nu(z,T))(1-2\nu(z,T))}, \tag{20}$$

$$C_{12}(z,T)=\frac{E(z,T)\nu(z,T)}{(1+\nu(z,T))(1-2\nu(z,T))}, \tag{21}$$

$$C_{66}(z,T)=\frac{E(z,T)}{2(1+\nu(z,T))}. \tag{22}$$

Thermal Analysis

In this study, the effect of a thermal environment on the free vibration behavior of the cantilever functionally graded plate which carrying a point mass is also investigated. In here the temperature distribution is considered as a nonlinear distribution that can be obtained by solving a steady-state heat transfer equation. The temperature distribution through the thickness is as follow [16],

$$-\frac{d}{dz}\left[\kappa(z)\frac{dT}{dz}\right] = 0,\ T = T_m \text{ at } z = -h/2;\ T = T_c \text{ at } z = h/2, \tag{23}$$

The solution of Eq. (23) is obtained using a polynomial series [16] as follow,

$$T(z) = T_0 + \Delta T\xi(z), \tag{24}$$

$$\xi(z) = \frac{1}{\delta}\left[\begin{array}{l}\left(\frac{2z+h}{2h}\right) - \frac{(\kappa_c-\kappa_m)}{(p+1)\kappa_m}\left(\frac{2z+h}{2h}\right)^{p+1} + \frac{(\kappa_c-\kappa_m)^2}{(2p+1)\kappa_m^2}\left(\frac{2z+h}{2h}\right)^{2p+1} \\ -\frac{(\kappa_c-\kappa_m)^3}{(3p+1)\kappa_m^3}\left(\frac{2z+h}{2h}\right)^{3p+1} + \frac{(\kappa_c-\kappa_m)^4}{(4p+1)\kappa_m^4}\left(\frac{2z+h}{2h}\right)^{4p+1} - \frac{(\kappa_c-\kappa_m)^5}{(5p+1)\kappa_m^5}\left(\frac{2z+h}{2h}\right)^{5p+1}\end{array}\right], \tag{25}$$

$$\delta = 1 - \frac{(\kappa_c-\kappa_m)}{(p+1)\kappa_m} + \frac{(\kappa_c-\kappa_m)^2}{(2p+1)\kappa_m^2} - \frac{(\kappa_c-\kappa_m)^3}{(3p+1)\kappa_m^3} + \frac{(\kappa_c-\kappa_m)^4}{(4p+1)\kappa_m^4} - \frac{(\kappa_c-\kappa_m)^5}{(5p+1)\kappa_m^5}, \tag{26}$$

In the comparison results, the uniform temperature distribution given as follow were used.

$$T = T_0 + \Delta T, \tag{27}$$

T_0 in Eqs. (24) and (27) is the room temperature with a value of 300 K and ΔT represents the temperature change. At nonlinear temperature distribution, the full metal bottom surface of the plate is assumed to be at T_0 temperature.

Thermal Stresses Based on Three-Dimensional Elasticity

The plate is initially stress-free at temperature T_0 and thermal stresses occur in the plate with temperature change. The initial stresses due to a temperature change of $\Delta T(z)$ are defined for a functionally graded plate as:

$$\sigma_i^T = -\left(C_{11}(z,T)\alpha(z,T) + C_{12}(z,T)\alpha(z,T)\right)\Delta T(z)(i = x, y), \tag{28}$$

Table 1 Boundary functions for considered boundary conditions

Boundary Condition	$f_U^1(X)$	$f_V^1(X)$	$f_W^1(X)$	$f_U^2(Y)$	$f_V^2(Y)$	$f_W^2(Y)$
C–C	$1-X^2$	$1-X^2$	$1-X^2$	$1-Y^2$	$1-Y^2$	$1-Y^2$
C–F	$1+X$	$1+X$	$1+X$	$1+Y$	$1+Y$	$1+Y$
F–F	1	1	1	1	1	1

Three-Dimensional Ritz Solution in Thermal Environment

The linear elastic strain potential energy U_s of the plate can be given as,

$$U_s = \frac{1}{2}\int_V \left[\sigma_x\varepsilon_x + \sigma_y\varepsilon_y + \sigma_z\varepsilon_z + \tau_{yz}\gamma_{yz} + \tau_{xz}\gamma_{xz} + \tau_{xy}\gamma_{xy}\right]dV, \tag{29}$$

The strain energy U_T from the initial stresses due to temperature rise can be given from Kim [17] as follow,

$$U_T = \frac{1}{2}\int_V \left[\sigma_x^T d_{xx} + 2\tau_{xy}^T d_{xy} + \sigma_y^T d_{yy}\right]dV, \tag{30}$$

$$d_{ij} = u_{,i}u_{,j} + v_{,i}v_{,j} + w_{,i}w_{,j}(i,j = x,y). \tag{31}$$

The kinetic energy T_p of the plate can be given as:

$$T_p = \frac{1}{2}\int_V \rho(z,T)\left[\left(\frac{\partial u}{\partial t}\right)^2 + \left(\frac{\partial v}{\partial t}\right)^2 + \left(\frac{\partial w}{\partial t}\right)^2\right]dV + \frac{1}{2}\sum_{p=1}^{N} m_p\left(\frac{\partial w}{\partial t}\right)^2, \tag{32}$$

The nondimensionalization process is performed using the following nondimensionalized parameters:

$$X = 2x/a;\ Y = 2y/b;\ Z = 2z/h, \tag{33}$$

According to thermal vibration problem the maximum energy functional Π of the elastic plate is defined as:

$$\Pi = \left(U_{smax} + U_{Tmax}\right) - T_{max}, \tag{34}$$

In here; U_{smax} is maximum of the nondimensionalized linear elastic strain potential energy, U_{Tmax} is maximum of the nondimensionalized thermal strain potential energy and T_{max} is maximum of the nondimensionalized kinetic energy and are obtained as follow:

$$U_{smax} = \frac{1}{2}\int_V \left[C_{11}\left(\varepsilon_x^2 + \varepsilon_y^2 + \varepsilon_z^2\right) + 2C_{12}\left(\varepsilon_x\varepsilon_y + \varepsilon_x\varepsilon_z + \varepsilon_y\varepsilon_z\right) + C_{66}\left(\gamma_{yz}^2 + \gamma_{xz}^2 + \gamma_{xy}^2\right)\right]dV, \tag{35}$$

$$U_{Tmax} = -\frac{1}{2}\int_V (C_{11} + C_{12})\alpha(z,T)\Delta T(z)\left[\left(\frac{\partial U}{\partial x}\right)^2 + \left(\frac{\partial V}{\partial x}\right)^2 + \left(\frac{\partial W}{\partial x}\right)^2 + \left(\frac{\partial U}{\partial y}\right)^2 + \left(\frac{\partial V}{\partial y}\right)^2 + \left(\frac{\partial W}{\partial y}\right)^2\right]dV, \tag{36}$$

$$T_{max} = \frac{\omega^2}{2}\int_V \rho(z,T)\left[U^2 + V^2 + W^2\right]dV + \frac{\omega^2}{2}\sum_{p=1}^{N} m_p W^2. \tag{37}$$

In this study, the Chebyshev polynomials are preferred which are the orthogonal polynomials reduced the computational effort [32]. In accordance with the Ritz method, each of the displacement amplitude functions is written as a triple series of Chebyshev polynomials, the displacement component of which is multiplied by a boundary function that satisfies the geometric boundary conditions of the plate. The displacement components are written in terms of nondimensionalized coordinates

Table 2 Coefficients of the temperature dependent material properties of constituents of FGM

Material	P_{-1}	P_0	P_1	P_2	P_3
Si_3N_4					
E (Pa)	0	348.43×10^9	-3.070×10^{-4}	2.160×10^{-7}	-8.946×10^{-11}
υ	0	0.2400	0	0	0
α (1/K)	0	5.8723×10^{-6}	9.095×10^{-4}	0	0
ρ (kg/m^3)	0	2370	0	0	0
κ (W/(mK))	0	9.19	0	0	0
SUS304					
E (Pa)	0	201.04×10^9	3.079×10^{-4}	-6.534×10^{-7}	0
υ	0	0.3262	-2.002×10^{-4}	3.797×10^{-7}	0
α (1/K)	0	12.330×10^{-6}	8.086×10^{-4}	0	0
ρ (kg/m^3)	0	8166	0	0	0
κ (W/(mK))	0	12.04	0	0	0

Table 3 Convergence and comparison of first five frequency parameters of cantilever isotropic plate without mass ($a/h=100$, $\Delta T=0$, $\upsilon=0.333$)

M	*a*/*b*	i× j×k	Nondimensionalized frequency parameters				
			Δ_1	Δ_2	Δ_3	Δ_4	Δ_5
0	1	4×4x4	3.5762	8.5140	21.9537	31.2937	31.9213
		5×5×5	3.5220	8.4768	21.6620	27.4786	31.4276
		6×6×6	3.5035	8.4216	21.3398	27.3788	30.8134
		7×7×7	3.4909	8.4042	21.2598	27.1042	30.7448
		8×8×8	3.4836	8.3879	21.2202	27.0913	30.6807
		Gorman [33]	3.459	8.356	21.09	27.06	30.55
	1.5	4×4×4	3.5906	6.4381	15.9983	23.0735	26.8188
		5×5×5	3.5392	6.3993	14.5051	22.5232	26.5504
		6×6×6	3.5221	6.3441	14.4817	22.1542	25.8724
		7×7×7	3.5087	6.3304	14.3039	22.0634	25.8141
		8×8×8	3.5016	6.3167	14.2936	22.0224	25.7172
		Gorman [33]	3.477	6.288	14.26	21.88	25.59
1	1	4×4×4	2.7821	8.5140	13.6886	26.1330	31.9213
		5×5×5	2.7374	8.4768	12.7961	23.6249	31.4276
		6×6×6	2.7138	8.4216	12.4247	23.5626	30.8134
		7×7×7	2.7008	8.4042	12.2086	23.2702	30.7448
		8×8×8	2.6946	8.3879	12.1549	23.2337	30.6807
		Chiba and Sugimoto [25]	2.732	8.502	12.996	23.745	31.153
		Aydoğdu and Filiz [28]	2.824	8.364	12.953	23.243	30.580

$$U(X,Y,Z) = F_u(X,Y)\sum_{i=1}^{\infty}\sum_{j=1}^{\infty}\sum_{k=1}^{\infty} A_{ijk}P_i(X)P_j(Y)P_k(Z), \tag{38}$$

$$V(X,Y,Z) = F_v(X,Y)\sum_{l=1}^{\infty}\sum_{m=1}^{\infty}\sum_{n=1}^{\infty} B_{lmn}P_l(X)P_m(Y)P_n(Z), \tag{39}$$

$$W(X,Y,Z) = F_w(X,Y)\sum_{p=1}^{\infty}\sum_{q=1}^{\infty}\sum_{r=1}^{\infty} C_{pqr}P_p(X)P_q(Y)P_r(Z), \tag{40}$$

where $P_s(\zeta) = \cos\left[(s-1)\arccos(\zeta)\right]$ ($s=1,2,3,\ldots;\ \zeta=X,Y,Z$) is the sth order one-dimensional Chebyshev polynomial and $F_\alpha(X,Y) = f_\alpha^1(X,Y)f_\alpha^2(X,Y)$ ($\alpha=U, V, W$) is the boundary function satisfying the geometric boundary conditions, are as follows in terms of nondimensionalized coordinates and Chebyshev polynomials. The boundary functions used for boundary condition in this study are given in the Table 1.

Table 4 Comparison of natural frequency parameters of clamped square functionally graded plates subjected to uniform temperature rise ($p=2$, $a/h=10$, $a=0.2$)

ΔT (K)	Source	Nondimensionalized frequency parameters				
		Δ_1	Δ_2	Δ_3	Δ_4	Δ_5
0	The rule of mixture	4.1249	7.8713	7.8713	11.0374	13.0130
	The Mori–Tanaka scheme	4.0787	7.7860	7.7860	10.9207	12.8766
	Kim [17]	4.1165	7.9696	7.9696	11.2198	13.1060
300	The rule of mixture	3.9872	7.6039	7.6039	10.6583	12.5629
	The Mori–Tanaka scheme	3.9537	7.5396	7.5396	10.5682	12.4557
	Kim [17]	3.6593	7.3098	7.3098	10.4021	12.1982
500	The rule of mixture	3.8241	7.2849	7.2849	10.2044	12.0227
	The Mori–Tanaka scheme	3.7889	7.2140	7.2140	10.1021	11.8986
	Kim [17]	3.2147	6.6561	6.6561	9.5761	11.2708

Table 5 Comparison of natural frequency parameters of clamped functionally graded plates subjected to non-linear temperature rise ($h/b=0.05$, $a/b=1$, $\Delta T=300$ K)

p	Source	Nondimensionalized frequency parameters				
		Δ_1	Δ_2	Δ_3	Δ_4	Δ_5
1	The Mori–Tanaka scheme	4.7964	9.5861	9.5861	13.8885	16.7426
	Li et al. [18]	4.4780	9.3453	9.3453	13.7358	16.6440
2	The Mori–Tanaka scheme	4.3394	8.6635	8.6635	12.5414	15.1109
	Li et al. [18]	3.9471	8.2896	8.2896	12.2071	14.8029
5	The Mori–Tanaka scheme	3.9678	7.9131	7.9131	11.4454	13.7834
	Li et al. [18]	3.4954	7.4142	7.4142	10.9500	13.2942
10	The Mori–Tanaka scheme	3.8012	7.5796	7.5796	10.9617	13.2005
	Li et al. [18]	3.3011	7.0428	7.0428	10.4184	12.6567

In accordance with the Ritz method, by substituting the displacement components given by Eq. (38)–(40) at the maximum energy values and substituting the maximum energy values in the maximum energy functional given by Eq. (34)–(37), the energy functional Π is obtained in terms of Chebyshev polynomials. Then the energy functional Π is minimized according to the unknown coefficients A_{ijk}, B_{lmn} and C_{pqr}.

$$\frac{\partial \prod}{\partial A_{ijk}} = 0, \tag{41}$$

$$\frac{\partial \prod}{\partial B_{lmn}} = 0, \tag{42}$$

$$\frac{\partial \prod}{\partial C_{pqr}} = 0. \tag{43}$$

As a result of the Ritz procedure, the eigenvalue problem given below is obtained, and the solution of the system of equations gives the natural frequencies of the free vibration problem occurring in the thermal environment under the influence of temperature.

$$\left(\begin{bmatrix} [K_{uu}] & [K_{uv}] & [K_{uw}] \\ [K_{uv}]^T & [K_{vv}] & [K_{vw}] \\ [K_{uw}]^T & [K_{vw}]^T & [K_{ww}] \end{bmatrix} - \Omega^2 \begin{bmatrix} [M_{uu}] & 0 & 0 \\ 0 & [M_{vv}] & 0 \\ 0 & 0 & [M_{ww}] \end{bmatrix}\right) \begin{Bmatrix} \{A_{ijk}\} \\ \{B_{lmn}\} \\ \{C_{pqr}\} \end{Bmatrix} = \begin{Bmatrix} \{0\} \\ \{0\} \\ \{0\} \end{Bmatrix}, \tag{44}$$

where $[K_{ij}]$ and $[M_{ij}]$ (i,j = u,v,w) are the stiffness matrix and diagonal mass matrix, respectively. The dimensionless coefficients $\{A_{ijk}\}$, $\{B_{lmn}\}$ and $\{C_{pqr}\}$ corresponding to the eigenvectors in the eigenvalue problem, represent the amplitude. Also, Ω is the nondimensional frequnecy parameter and obtained as:

$$\Omega = \omega\left(a^2/h\right)\sqrt{\rho_{m0}/E_{m0}}, \tag{45}$$

Here ω is the natural frequency and ρ_{m0} and E_{m0} are mass density per unit volume and Young modulus of metal at room temperature ($T_0=300$ K).

Table 6 Frequency parameters of cantilever functionally graded plates with various temperature differences ($a/h = 10$, $a/b = 1$)

ΔT	Material composition	Nondimensionalized frequency parameters					
		Δ_1	Δ_2	Δ_3	Δ_4	Δ_5	Δ_6
Without mass							
0	Si_3N_4	7.5478	18.6562	45.0671	49.6717	56.6032	64.5702
	1	4.6859	11.1744	27.6203	30.1946	34.8129	39.0427
	2	4.2384	10.0337	24.8961	26.8167	31.4358	35.0865
	5	3.8777	9.1135	22.7002	24.0644	28.7171	31.8948
	10	3.7137	8.6863	21.7021	22.9632	27.4868	30.4455
	SUS304	3.4822	8.0576	20.2715	21.7607	25.7495	28.3671
300	Si_3N_4	7.4638	18.4008	44.5543	49.0469	55.9659	63.7579
	1	4.6316	11.0248	27.3079	29.7954	34.4399	38.5710
	2	4.1869	9.8950	24.6042	26.4506	31.0875	34.6504
	5	3.8250	8.9748	22.4048	23.7170	28.3635	31.4587
	10	3.6583	8.5421	21.3913	22.6175	27.1138	29.9905
	SUS304	3.4182	7.8966	19.9143	21.4080	25.3174	27.8545
500	Si_3N_4	7.4145	18.2536	44.2584	48.6877	55.5991	63.2917
	1	4.5916	10.9146	27.0755	29.4728	34.1624	38.2192
	2	4.1442	9.7795	24.3567	26.1075	30.7917	34.2790
	5	3.7729	8.8360	22.1013	23.3279	27.9988	31.0089
	10	3.5959	8.3780	21.0274	22.1935	26.6747	29.4572
	SUS304	3.3285	7.6679	19.3937	20.9251	24.6848	27.1089
With point mass M = 1 (X,Y) = (1,0)							
0	Si_3N_4	1.6530	18.6562	26.5406	49.6717	52.5775	64.5702
	1	1.4826	11.1744	16.3934	30.1946	32.6968	39.0427
	2	1.4448	10.0337	14.8240	26.8167	29.5537	35.0865
	5	1.4072	9.1135	13.5550	24.0644	27.0217	31.8948
	10	1.3819	8.6863	12.9701	22.9632	25.8951	30.4455
	SUS304	1.3306	8.0576	12.1105	21.7607	24.3374	28.3671
300	Si_3N_4	1.6339	18.4008	26.2034	49.0469	52.0339	63.7579
	1	1.4648	11.0248	16.1906	29.7954	32.3634	38.5710
	2	1.4266	9.8950	14.6355	26.4506	29.2405	34.6504
	5	1.3874	8.9748	13.3661	23.7170	26.7027	31.4587
	10	1.3605	8.5421	12.7730	22.6175	25.5576	29.9905
	SUS304	1.3054	7.8966	11.8882	21.4080	23.9438	27.8545
500	Si_3N_4	1.6227	18.2536	26.0101	48.6877	51.7198	63.2917
	1	1.4517	10.9146	16.0407	29.4728	32.1136	38.2192
	2	1.4116	9.7795	14.4766	26.1075	28.9720	34.2790
	5	1.3679	8.8360	13.1731	23.3279	26.3704	31.0089
	10	1.3366	8.3780	12.5436	22.1935	25.1575	29.4572
	SUS304	1.2702	7.6679	11.5649	20.9251	23.3662	27.1089

Numerical Results

In this study, silicon nitride (Si3N4) as ceramic phase and stainless steel (SUS304) as metal phase are chosen to be the constituent materials of the functionally graded plate. Mechanical properties of constituent materials are temperature dependent as follows:

$$P(T) = P_0\left(P_{-1}T^{-1} + 1 + P_1T + P_2T^2 + P_3T^3\right), \qquad (46)$$

Table 7 Frequency parameters of cantilever functionally graded plates with various temperature differences ($a/h = 10$, $a/b = 1.5$)

ΔT	Material composition	Nondimensionalized frequency parameters					
		Δ_1	Δ_2	Δ_3	Δ_4	Δ_5	Δ_6
Without mass							
0	Si_3N_4	7.5315	25.0474	39.6468	45.1831	80.9517	108.8917
	1	4.6624	14.9073	24.3014	27.7972	48.5035	66.1242
	2	4.2146	13.3756	21.6061	25.0748	43.5245	59.6283
	5	3.8534	12.1470	19.3930	22.8817	39.5208	54.4735
	10	3.6886	11.5770	18.5066	21.8927	37.6970	52.1277
	SUS304	3.4540	10.7309	17.5457	20.4944	35.0542	48.6568
300	Si_3N_4	7.4463	24.6948	39.1663	44.6801	79.8811	107.6174
	1	4.6074	14.7054	23.9840	27.4925	47.8987	65.4122
	2	4.1623	13.1884	21.3142	24.7899	42.9676	58.9657
	5	3.8000	11.9592	19.1163	22.5932	38.9646	53.7948
	10	3.6324	11.3811	18.2318	21.5888	37.1173	51.4012
	SUS304	3.3892	10.5120	17.2666	20.1440	34.4045	47.8030
500	Si_3N_4	7.3963	24.4912	38.8897	44.3899	79.2676	106.8827
	1	4.5668	14.5559	23.7280	27.2654	47.4468	64.8759
	2	4.1190	13.0316	21.0411	24.5477	42.4922	58.3946
	5	3.7472	11.7707	18.8066	22.2955	38.3901	53.0866
	10	3.5691	11.1582	17.8950	21.2317	36.4380	50.5401
	SUS304	3.2985	10.2023	16.8850	19.6326	33.4608	46.5480
With point mass M = 1 (X,Y) = (1,0)							
0	Si_3N_4	1.6690	25.0474	30.1036	39.6468	74.2003	80.9517
	1	1.4937	14.9073	18.7513	24.3014	45.5607	48.5035
	2	1.4547	13.3756	16.9753	21.6061	41.0260	43.5245
	5	1.4159	12.1470	15.5386	19.3930	37.3548	39.5208
	10	1.3898	11.5770	14.8837	18.5066	35.7151	37.6970
	SUS304	1.3369	10.7309	13.9385	17.5457	33.3955	35.0542
300	Si_3N_4	1.6496	24.6948	29.7452	39.1663	73.2773	79.8811
	1	1.4756	14.7054	18.5322	23.9840	45.0122	47.8987
	2	1.4362	13.1884	16.7708	21.3142	40.5174	42.9676
	5	1.3958	11.9592	15.3326	19.1163	36.8463	38.9646
	10	1.3681	11.3811	14.6679	18.2318	35.1849	37.1173
	SUS304	1.3113	10.5120	13.6925	17.2666	32.7975	34.4045
500	Si_3N_4	1.6383	24.4912	29.5394	38.8897	72.7480	79.2676
	1	1.4622	14.5559	18.3696	23.7280	44.5997	47.4468
	2	1.4209	13.0316	16.5976	21.0411	40.0790	42.4922
	5	1.3759	11.7707	15.1206	18.8066	36.3149	38.3901
	10	1.3437	11.1582	14.4148	17.8950	34.5576	36.4380
	SUS304	1.2754	10.2023	13.3330	16.8850	31.9261	33.4608

where P_0 is the material property of ceramic and metal at temperature T_0, respectively. P_0 and the coefficients of material properties depending on temperature, P_i ($i = 0,1,2,3$) are given in Table 2 [17, 18].

Convergence and Accuracy Studies

In this study, the natural frequencies are obtained by Ritz method. The number of terms of the Chebyshev

Table 8 Frequency parameters of cantilever functionally graded plates with various temperature differences ($a/h=10$, $a/b=2$)

ΔT	Material composition	Nondimensionalized frequency parameters					
		Δ_1	Δ_2	Δ_3	Δ_4	Δ_5	Δ_6
Without mass							
0	Si_3N_4	7.5186	31.0010	32.4327	45.1532	97.2486	116.5419
	1	4.6441	18.0522	20.3395	27.7576	57.8121	71.3537
	2	4.1961	16.2094	18.0716	25.0354	51.8488	63.7755
	5	3.8346	14.8223	16.1063	22.8423	47.0979	57.6096
	10	3.6691	14.2061	15.2829	21.8524	44.9318	55.1246
	SUS304	3.4321	13.2147	14.4350	20.4506	41.7464	52.3863
300	Si_3N_4	7.4324	30.5542	32.0496	44.6482	95.9236	115.2220
	1	4.5885	17.8317	20.0454	27.4521	57.0902	70.5340
	2	4.1432	16.0058	17.7997	24.7497	51.1853	63.0038
	5	3.7807	14.6138	15.8515	22.5530	46.4321	56.8502
	10	3.6123	13.9786	15.0394	21.5477	44.2343	54.3557
	SUS304	3.3667	12.9404	14.2078	20.0996	40.9609	51.5825
500	Si_3N_4	7.3818	30.2946	31.8304	44.3568	95.1643	114.4600
	1	4.5475	17.6633	19.8151	27.2243	56.5478	69.8704
	2	4.0995	15.8295	17.5538	24.5069	50.6154	62.2748
	5	3.7273	14.3999	15.5741	22.2546	45.7417	55.9907
	10	3.5485	13.7160	14.7470	21.1898	43.4154	53.4030
	SUS304	3.2754	12.5509	13.9017	19.5872	39.8201	50.4706
With point mass M = 1 (X,Y) = (1,0)							
0	Si_3N_4	1.6722	31.0010	31.0779	32.4327	84.6825	97.2486
	1	1.4939	18.0522	19.3981	20.3395	52.1730	57.8121
	2	1.4543	16.2094	17.5649	18.0716	46.9598	51.8488
	5	1.4148	14.8223	16.0814	16.1063	42.7192	47.0979
	10	1.3883	14.2061	15.2829	15.4065	40.8369	44.9318
	SUS304	1.3343	13.2147	14.4350	14.4377	38.2014	41.7464
300	Si_3N_4	1.6527	30.5542	30.7165	32.0496	83.6062	95.9236
	1	1.4756	17.8317	19.1758	20.0454	51.5297	57.0902
	2	1.4356	16.0058	17.3570	17.7997	46.3639	51.1863
	5	1.3945	14.6138	15.8515	15.8714	42.1248	46.4321
	10	1.3663	13.9786	15.0394	15.1861	40.2181	44.2343
	SUS304	1.3084	12.9404	14.1852	14.2078	37.5054	40.9609
500	Si_3N_4	1.6412	30.2946	30.5086	31.8304	82.9897	95.1643
	1	1.4621	17.6633	19.0107	19.8151	51.0442	56.5478
	2	1.4201	15.8295	17.1806	17.5538	45.8471	50.6154
	5	1.3744	14.3999	15.5741	15.6549	41.4993	45.7417
	10	1.3417	13.7160	14.7470	14.9271	39.4821	43.4154
	SUS304	1.2722	12.5509	13.8158	13.9017	36.4909	39.8201

polynomials used as admissible functions is decided by comparing the results for isotropic plate results which presented by Gorman [33] in the case of without mass and which presented by Chiba and Sugimoto [25] and Aydoğdu and Filiz [28] in the case of with mass. As the results were found to be in good agreement, it was concluded that it would be appropriate to determine the term number

Table 9 Frequency parameters of cantilever functionally graded plates with various mass ratios and various mass locations ($p=2$, $a/h=10$, $\Delta T=300$, $a/b=1$)

(X,Y)	M	Nondimensionalized frequency parameters					
		Δ_1	Δ_2	Δ_3	Δ_4	Δ_5	Δ_6
(− 0.5,0)	0.1	4.1715	9.8950	23.3216	26.4506	29.6603	34.6504
	0.2	4.1561	9.8950	21.5774	26.4506	28.6197	34.6504
	0.5	4.1090	9.8950	17.0366	26.4506	27.5051	34.6504
	1	4.0286	9.8950	13.1916	26.4506	27.1156	34.6504
(0,0)	0.1	4.0187	9.8950	21.5839	26.4506	28.1868	34.6504
	0.2	3.8656	9.8950	19.0337	26.4506	27.5499	34.6504
	0.5	3.4820	9.8950	15.2987	26.4506	27.1394	34.6504
	1	3.0223	9.8950	13.1045	26.4506	27.0056	34.6504
(0.5,0)	0.1	3.6538	9.8950	24.5243	26.4506	26.8244	34.6504
	0.2	3.2800	9.8950	24.1211	25.1397	26.4506	34.6504
	0.5	2.6037	9.8950	22.0275	24.7413	26.4506	34.6504
	1	2.0460	9.8950	20.7807	24.7090	26.4506	34.6504
(1,0)	0.1	3.1770	9.8950	18.2137	26.4506	29.5561	34.6504
	0.2	2.6521	9.8950	16.5590	26.4506	29.3914	34.6504
	0.5	1.9146	9.8950	15.1822	26.4506	29.2799	34.6504
	1	1.4266	9.8950	14.6355	26.4506	29.2405	34.6504

Table 10 Frequency parameters of cantilever functionally graded plates with various mass ratios and various mass locations ($p=2$, $a/h=10$, $\Delta T=300$, $a/b=1.5$)

(X,Y)	M	Nondimensionalized frequency parameters					
		Δ_1	Δ_2	Δ_3	Δ_4	Δ_5	Δ_6
(− 0.5,0)	0.1	4.1472	13.1884	21.3142	23.3182	42.9676	50.5889
	0.2	4.1320	13.1884	21.3142	21.8194	42.9676	44.1385
	0.5	4.0862	13.1884	18.0860	21.3142	37.3096	42.9676
	1	4.0092	13.1884	14.4675	21.3142	34.6805	42.9676
(0,0)	0.1	3.9980	13.1884	21.3142	21.7064	42.9676	53.4051
	0.2	3.8490	13.1884	19.6536	21.3142	42.9676	50.2540
	0.5	3.4772	13.1884	16.4305	21.3142	42.9676	46.7492
	1	3.0313	13.1884	14.3264	21.3142	42.9676	45.1562
(0.5,0)	0.1	3.6389	13.1884	21.3142	24.7330	42.9676	50.9037
	0.2	3.2723	13.1884	21.3142	24.6904	42.9676	45.7788
	0.5	2.6068	13.1884	21.3142	24.6096	39.9988	42.9676
	1	2.0544	13.1884	21.3142	24.5432	37.2016	42.9676
(1,0)	0.1	3.1702	13.1884	20.0960	21.3142	42.9676	44.8823
	0.2	2.6539	13.1884	18.6435	21.3142	42.6212	42.9676
	0.5	1.9234	13.1884	17.3242	21.3142	41.0662	42.9676
	1	1.4362	13.1884	16.7708	21.3142	40.5174	42.9676

Table 11 Frequency parameters of cantilever functionally graded plates with various mass ratios and various mass locations ($p=2$, $a/h=10$, $\Delta T=300$, $a/b=2$)

(X,Y)	M	Nondimensionalized frequency parameters					
		Δ_1	Δ_2	Δ_3	Δ_4	Δ_5	Δ_6
(− 0.5,0)	0.1	4.1284	16.0058	17.7997	23.2606	51.1853	54.8487
	0.2	4.1136	16.0058	17.7997	21.8305	48.5803	51.1853
	0.5	4.0689	16.0058	17.7997	18.3700	41.2155	51.1853
	1	3.9942	14.9243	16.0058	17.7997	37.9831	51.1853
(0,0)	0.1	3.9812	16.0058	17.7997	21.6370	51.1853	62.9492
	0.2	3.8345	16.0058	17.7997	19.6577	51.1853	62.8874
	0.5	3.4681	16.0058	16.5717	17.7997	51.1853	62.6523
	1	3.0279	14.5307	16.0058	17.7997	51.1853	62.1353
(0.5,0)	0.1	3.6246	16.0058	17.7997	24.6661	51.1853	59.9751
	0.2	3.2612	16.0058	17.7997	24.6091	51.1853	56.0777
	0.5	2.6007	16.0058	17.7997	24.5124	50.3203	51.1853
	1	2.0512	16.0058	17.7997	24.4420	47.1472	51.1853
(1,0)	0.1	3.1598	16.0058	17.7997	20.4533	51.1853	51.9407
	0.2	2.6476	16.0058	17.7997	19.1202	49.1517	51.1853
	0.5	1.9212	16.0058	17.7997	17.8841	47.1095	51.1853
	1	1.4356	16.0058	17.3570	17.7997	46.3639	51.1853

of Chebyshev polynomials in all directions equal number as $8\times8\times8$ as seen in Table 3. However, computational optimization could be obtained using unequal number of series terms in all directions.

Tables 4 and 5 show that the results for the clamped square functionally grade plates subjected the uniform temperature distribution and nonlinear temperature distribution, respectively are in good agreement as with presented by Kim [17] and Li et al. [18].

Parametric Studies

The object of this study is determined to effects of the mass ratio and location of the point mass on frequency parameters that moderately thick ($a/h=10$) functionally graded plates with and without thermal environment. In the results the values of side to side ratios are $a/b=1$; 1.5 and 2, volume fraction exponents are $p=1$, 2, 5 and 10 and temperature differences are $\Delta T=0$, 300 and 500 K are considered. The temperature distribution is considered as in the form of nonlinear. The results are presented as for with a point mass that mass ratio $M=0.1$, 0.2, 0.5 and 1 and without mass. The location coordinates of point mass are presented as (X,Y) = (− 0.5,0); (0,0); (0.5,0); (1,0) in the tables. And to see the case of different locations according to y axis the location coordinates of point mass are presented as (X,Y) = (0,0); (1,0); (–0 .5,0.5); (0.5,– 0.5) in the mod shape figures. The location of the point mass was determined according to whether the coordinates were on the symmetry axis or not according to the boundary condition considered. Here, the (1,0) and (0,0) coordinates are above the symmetry axis according to the considered boundary condition. And also the (0,0) coordinates are correspond the geometric center of the plate. The (− 0.5,0.5) ve (0.5,− 0.5) coordinates are not above the axis that is symmetrical with respect to the considered boundary condition. Thus, it provides a better understanding of the effects of the point mass whether on the symmetry axis or not on the frequency parameters.

Tables 6, 7 and 8 presents the frequency parameters obtained for the cases of with and without mass depending on the volume fraction exponent p and temperature differences for $a/b=1$, 1.5 and 2, respectively. For the cases with point mass, the location of point mass is considered as (1,0). According to these results free vibration frequencies decreases with increasing p index and temperature difference. The frequencies obtained according to the with point mass cases are always smaller than the frequency values obtained for the without point mass case. One can be seen that from Tables 6, 7 and 8, when the $a/b=1$, the second, the fourth and the sixth frequencies remain constant

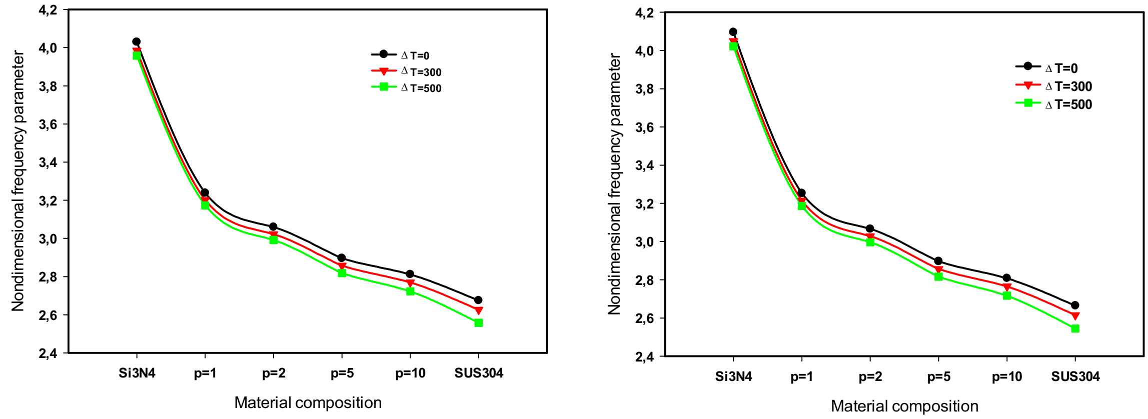

(a) a/b=1 **(b) a/b=2**

Fig. 2 Variation of fundamental frequency parameter with temperature differences for cantilever functionally graded plate with point mass ($a/h = 10$, $(X,Y) = (0,0)$)

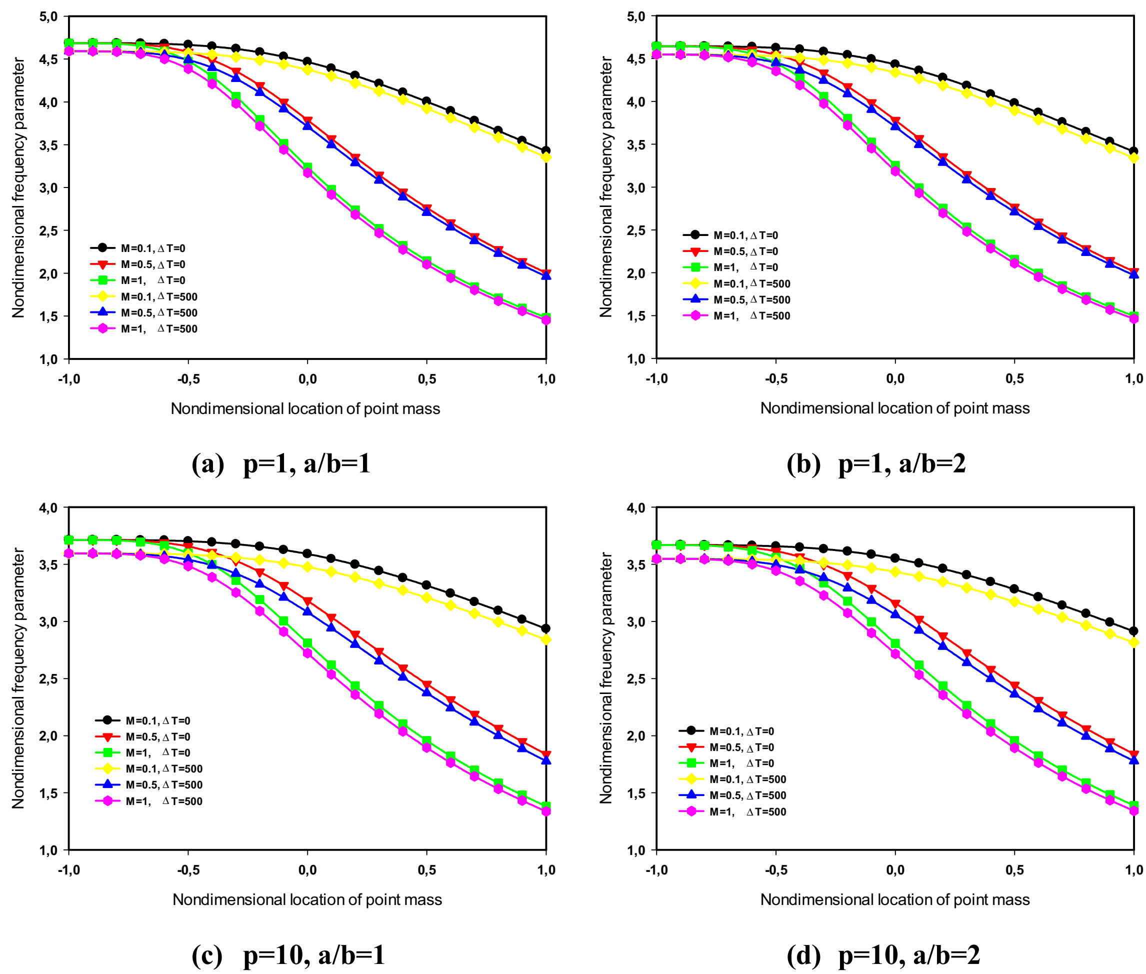

Fig. 3 Variation of fundamental frequency parameter with the location of point mass throguhout x axis for cantilever functionally graded plate with point mass ($a/h = 10$, Y = 0)

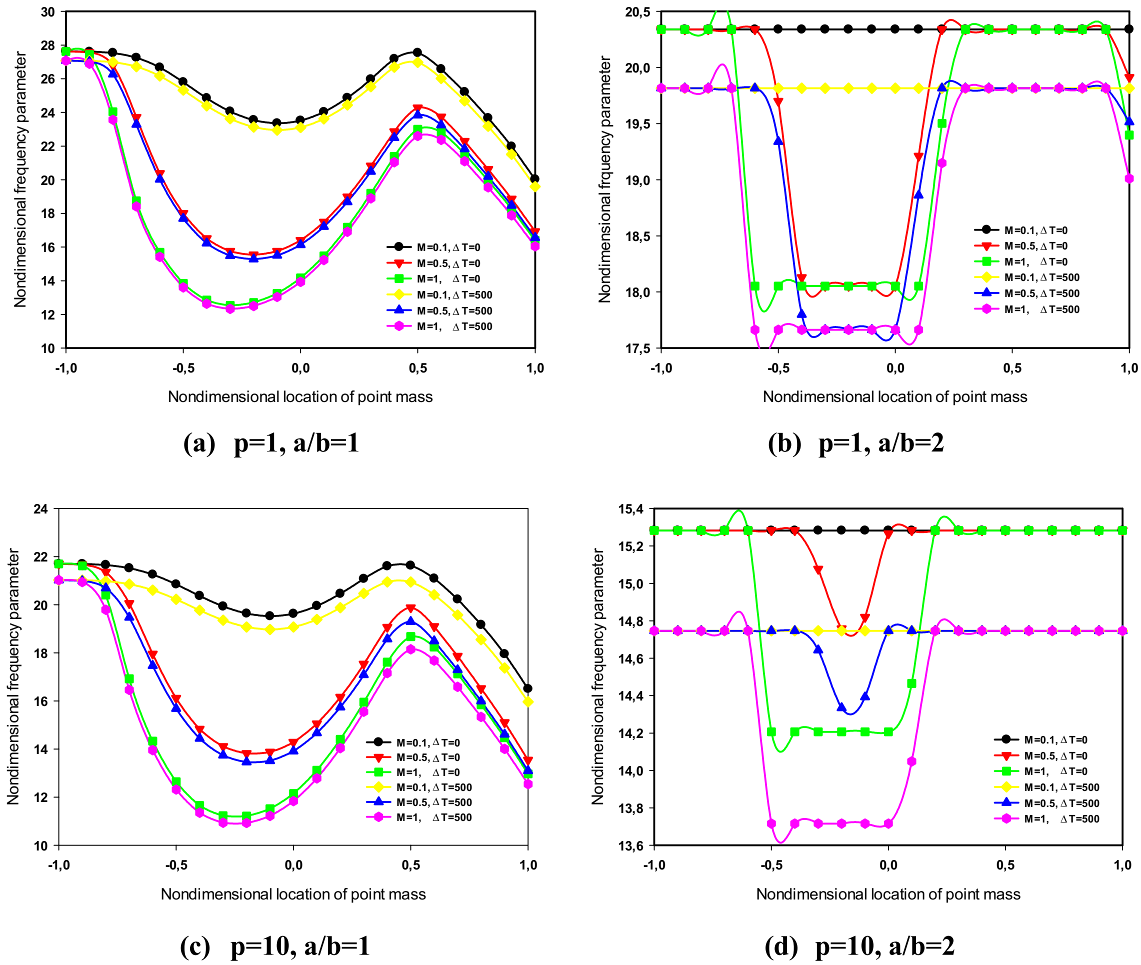

Fig. 4 Variation of third frequency parameter with the location of point mass throguhout x axis for cantilever functionally graded plate with point mass ($a/h=10$, $Y=0$)

as independent of the presence of mass. At the values of $a/b=1.5$ and 2, it is seen that the second frequencies remain constant as independent from the presence of mass. It means that the mass does not move during these vibrations because of the mass is at a nodal line. However, when the $a/b=1{,}5$ and 2, it is seen that at high frequencies, intermediate frequencies occur in the case of with mass. As a result of this, in the case of without mass the third and the fifth frequencies, respectively, appears to be equivalent in the case of with mass to the fourth and sixth frequencies. It means that the case of with point mass the nodal lines are displaced.

Tables 9, 10 and 11 presents the frequency parameters obtained for in the case of for different location of the point mass throughout the x axis for different mass rate from 0.1 to 1, for $a/b=1$, 1.5 and 2, respectively. It is seen that when the point mass is located at symmetry axis according the boundary condition which correspond $Y=0$ and throughout the x axis; some frequencies remain constant independent of the increasing of mass ratios because

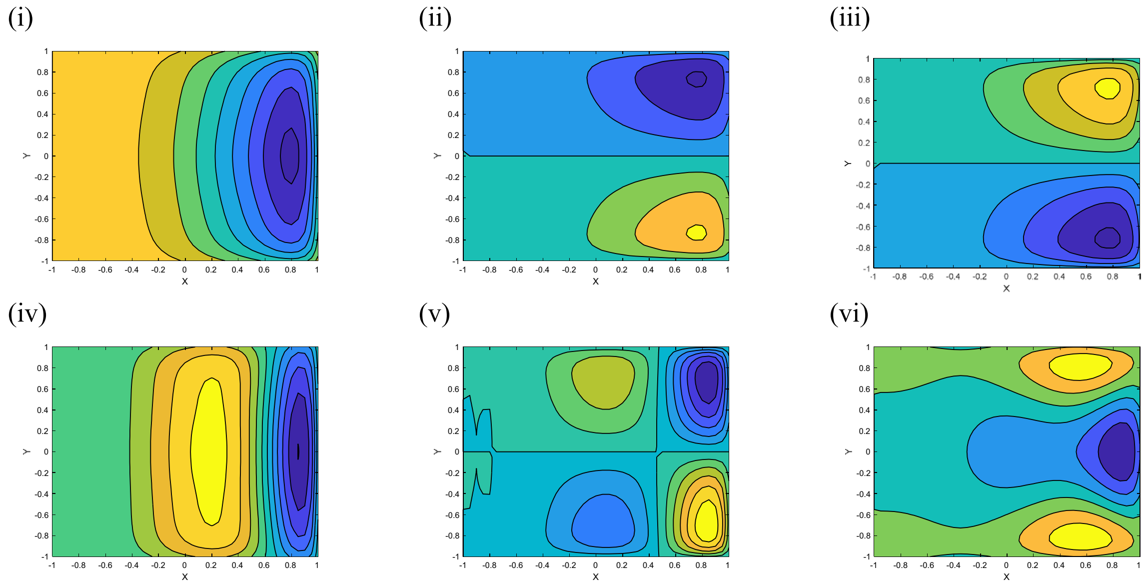

(a) ΔT=0 K (i)4.2146, (ii)13.3756, (iii)21.6061, (iv)25.0748, (v)43.5245, (vi)59.6283

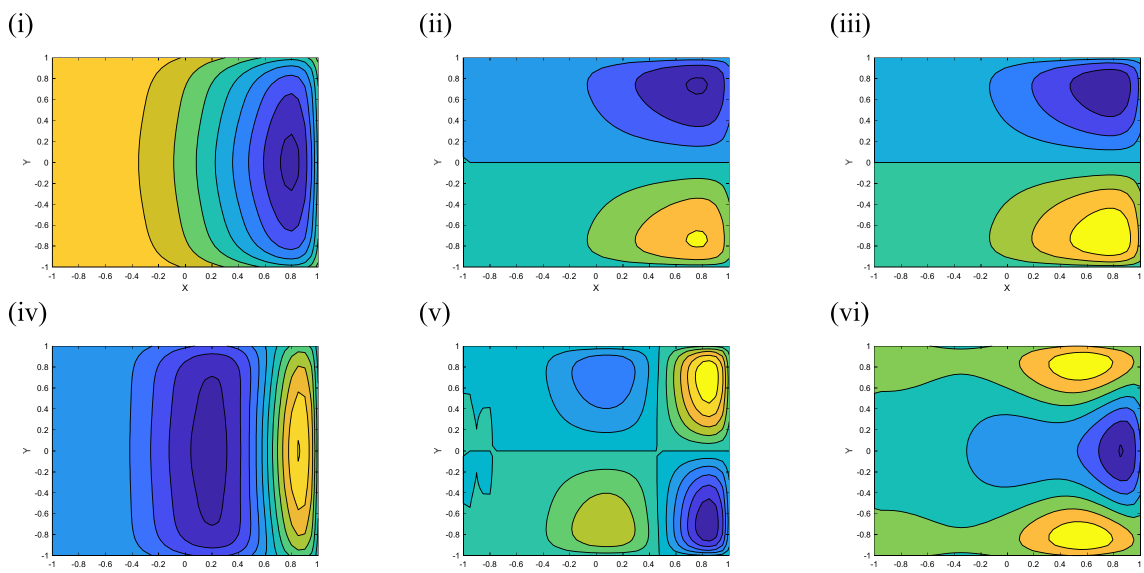

(b) ΔT=500 K (i)4.1190, (ii)13.0316, (iii)21.0411, (iv)24.5477, (v)42.4922, (vi)58.3946

Fig. 5 First six mode shapes of cantilever functionally graded plate without mass ($p=2$, $a/b=1.5$, $a/h=10$)

of the mass is at a nodal line and the mass dos not move during these vibrations.

Variation of fundamental frequency parameter with volume fraction index for various temperature differences for cantilever functionally graded plate with point mass on plate center are given in Fig. 2. Generally the effect of temperature on frequency parameter higher at higher volume fraction index. Also, The effect of volume fraction index on

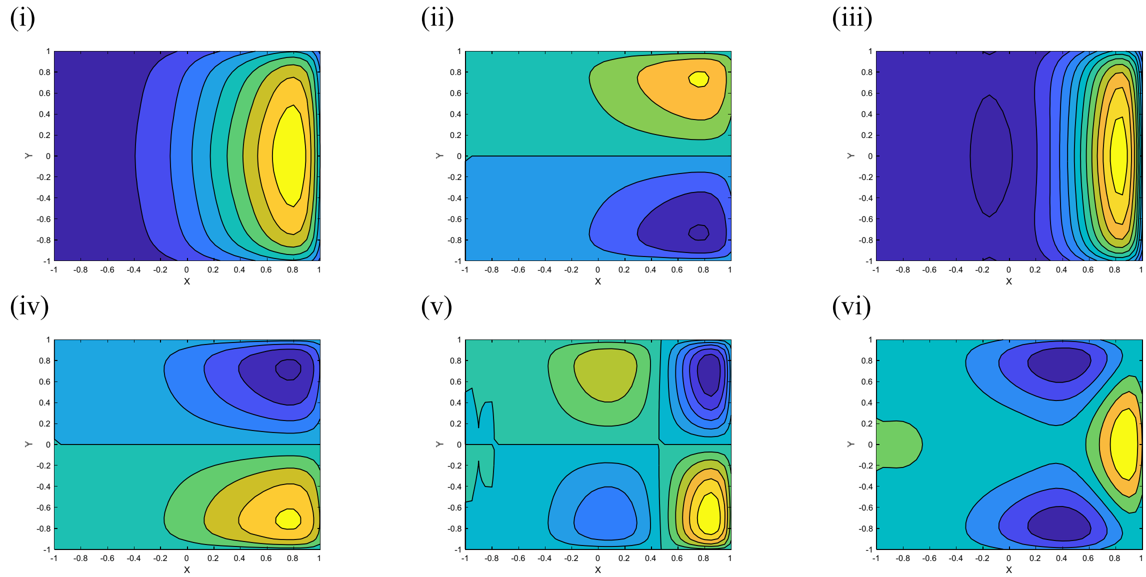

(a) ΔT=0 K (i)3.0689, (ii)13.3756, (iii)14.4752, (iv)21.6061, (v)43.5245, (vi)45.6702

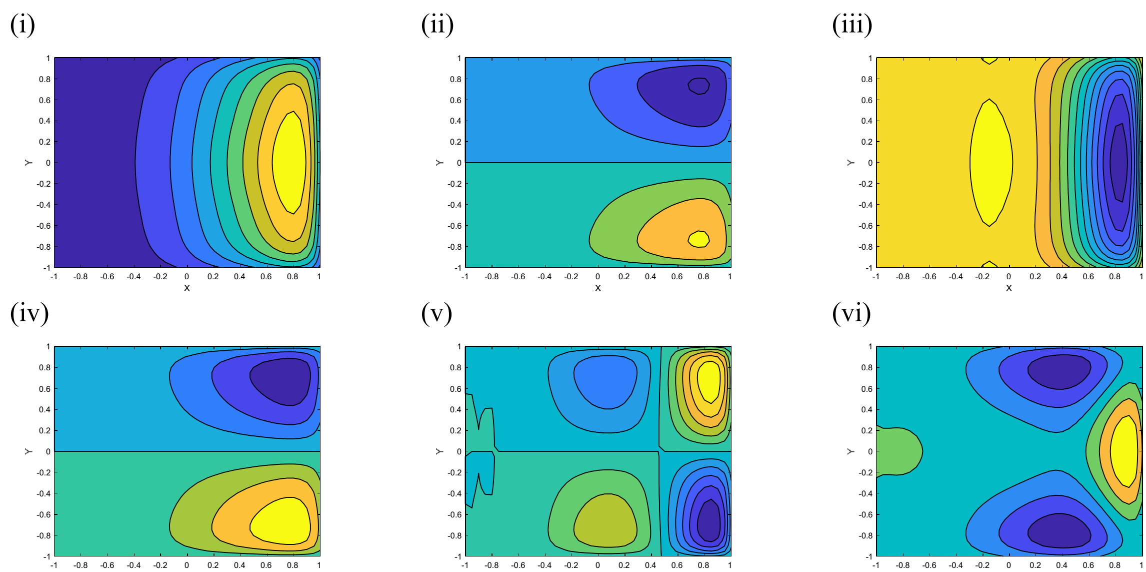

(b) ΔT=500 K (i)3.0000, (ii)13.0316, (iii)14.1985, (iv)21.0411, (v)42.4922, (vi)44.7129

Fig. 6 First six mode shapes of cantilever functionally graded plate with point mass ($p=2$, $a/b=1.5$, $a/h=10$, $M=1$, (X,Y) = (0,0))

frequency parameter higher decreasing with increasing of volume fraction index.

Effect of the location of point mass throguhout x axis for cantilever functionally graded plate for different point mass ratio and for various temperature differences on fundamental frequency parameter and on third frequency parameter are given in Figs. 3 and 4, respectively. For all considered mass ratios, the fundamental frequency remains almost unchanged when the point mass is near the clamped edge,

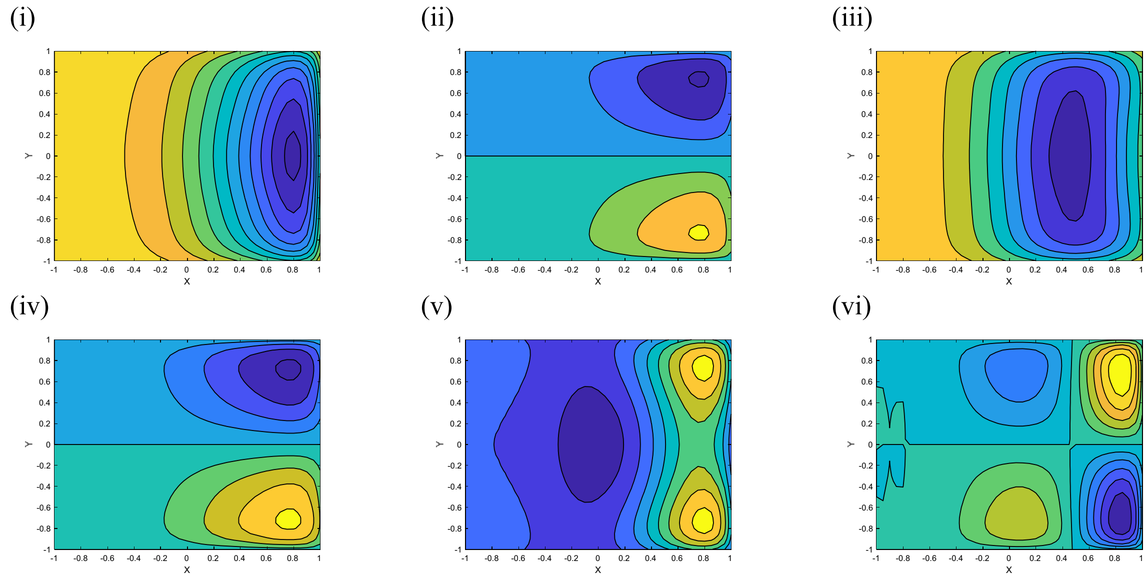

(a) ΔT=0 K (i)1.4547, (ii)13.3756, (iii)16.9753, (iv)21.6061, (v)41.0260, (vi)43.5245

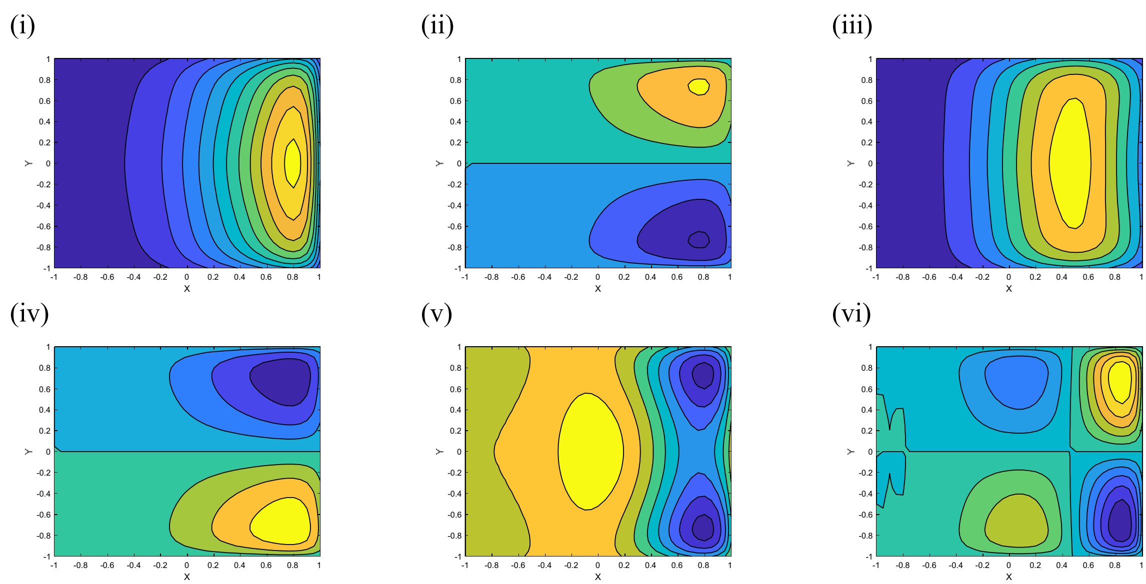

(b) ΔT=500 K (i)1.4209, (ii)13.0316, (iii)16.5976, (iv)21.0411, (v)40.0790, (vi)42.4922

Fig. 7 First six mode shapes of cantilever functionally graded plate with point mass (p = 2, a/b = 1.5, $a/h = 10$, $M = 1$, $(X,Y) = (1,0)$)

while it decreases substantially as the point mass approaches the free edge. Finally, the fundamental frequency reaches its minimum value at the free edge for all considered mass ratios, temperature differences, p values and a/b ratios. The decreasing on fundamental frequency parameters are greater with increasing mass ratios. It can be seen that the change of the third mode at different mass ratios along the x-axis is in the waveform for $a/b = 1$. The frequency parameters reaches a maximum value on a point which shifts gradually outward with increasing mass ratios. For $a/b = 2$ ratio, it is seen that the change in the position of the point mass along x axis, the effect on the frequency remains constant locally and has a sharp effect on the frequency change at some critical points. It is seen that the frequency values obtained by considering the temperature effect are always lower than the frequency

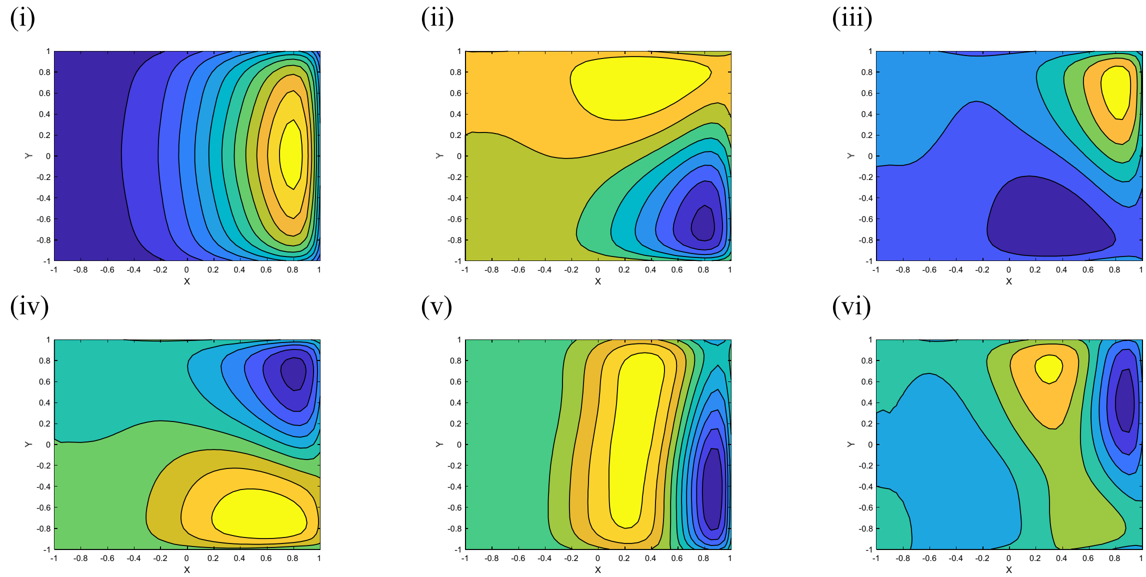

(a) ΔT=0 K (i)4.0630, (ii)11.2423, (iii)16.0725, (iv)21.6095, (v)32.6159, (vi)49.5791

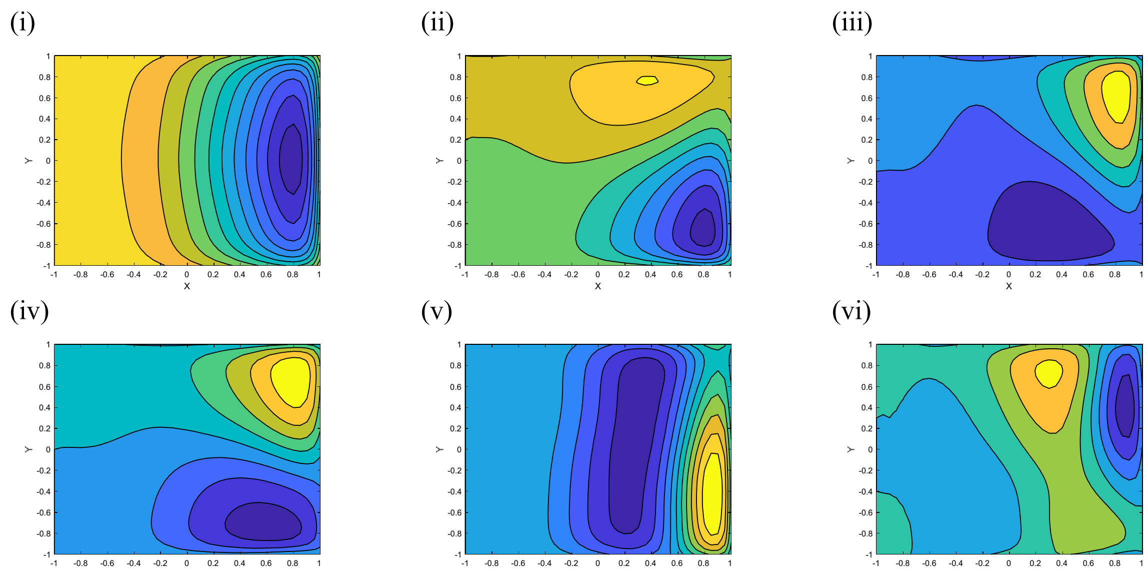

(b) ΔT=500 K (i)3.9712, (ii)10.9756, (iii)15.7150, (iv)21.0437, (v)31.9130, (vi)48.4637

Fig. 8 First six mode shapes of cantilever functionally graded plate with point mass ($p=2$, $a/b=1.5$, $a/h=10$, $M=1$, $(X,Y)=(-0.5,0.5)$)

values obtained at room temperature, and the change always remains parallel to each other.

The mod shapes for the first six frequencies of plate for p value is 2, side to side ratio a/b is 1.5 and mass ratio is 1 are presented with Figs. 5, 6, 7, 8 and 9. These figures are presented for in the case of without mass and drawn for in the case of with mass four different locations of point mass and the conditions where the temperature difference is 0 and 500 K, respectively. Whether the cases where the point mass is on the axis of symmetry, the mode shapes maintain their symmetry with respect to the axis. It is seen that the nodal lines changing at the points where the mass is outside the symmetry axis and some modes shifting. On the other hand, it is seen that the temperature to cause waves to change phase in some modes.

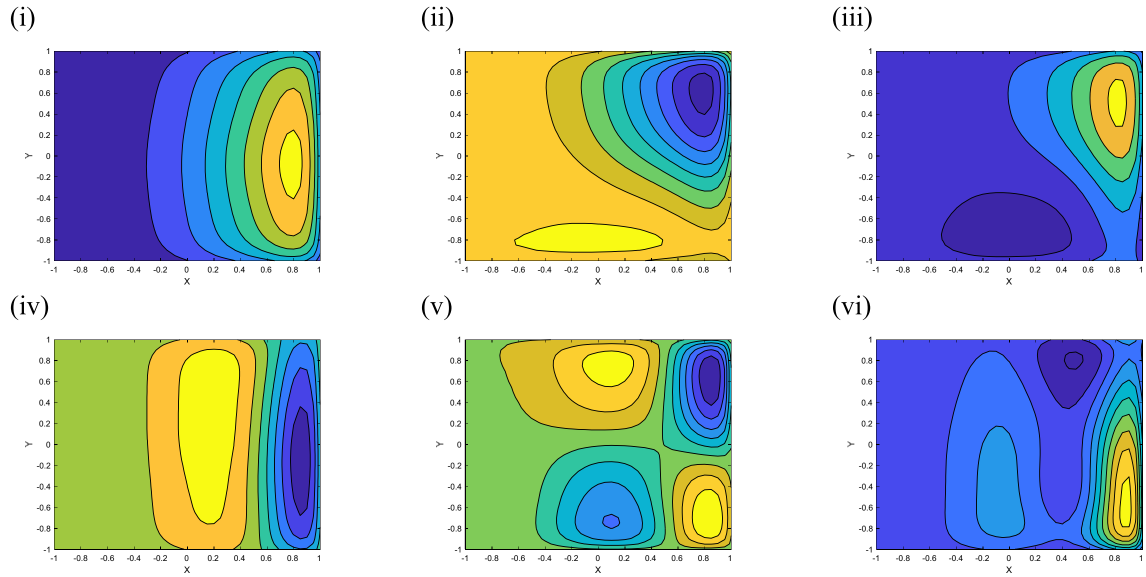

(a) ΔT=0 K (i)2.0429, (ii)10.8116, (iii)21.5683, (iv)24.8724, (v)43.2668, (vi)52.6142

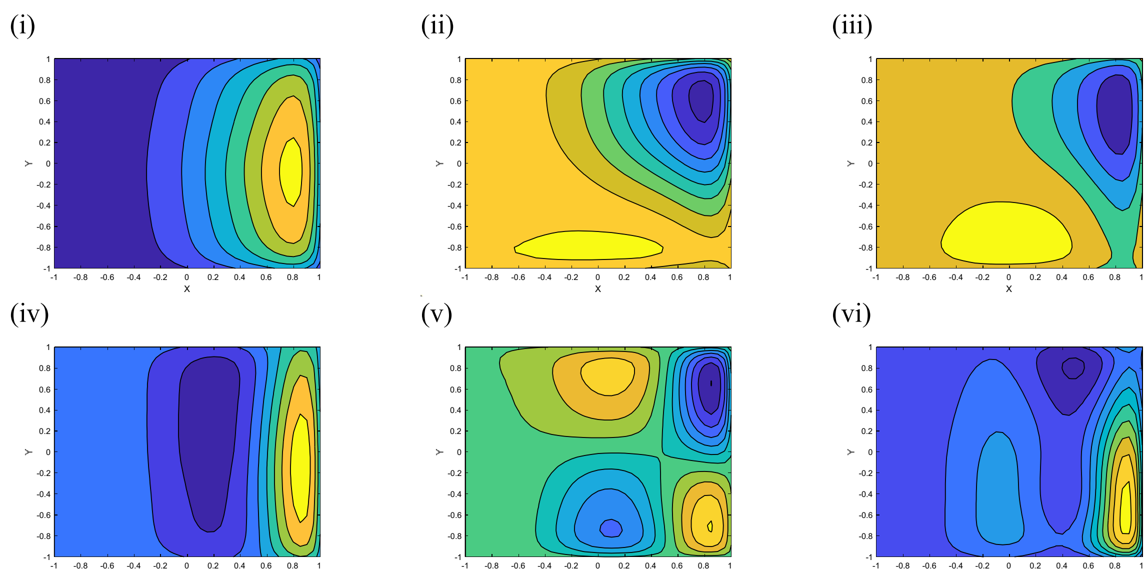

(b) ΔT=500 K (i)1.9964, (ii)10.5344, (iii)21.0115, (iv)24.3495, (v)42.2477, (vi)51.5980

Fig. 9 First six mode shapes of cantilever functionally graded plate with point mass ($p=2$, $a/b=1.5$, $a/h=10$, $M=1$, $(X,Y)=(0.5,-0.5)$)

Conclusions

The free vibration has been performed on a cantilever functionally graded plate carrying a point mass on an arbitrary point using Ritz method based on three-dimensional elasticity under nonlinear temperature distribution. The effective material properties are estimated by Mori–Tanaka homogenization scheme. The following conclusions can be reached as a result of the analysis.

- Choosing the terms number of Chebyshev polynomials which used as admissible functions in Ritz method as $8 \times 8 \times 8$, the results can be obtained in good agreement with literature and consitent.

- Free vibration frequencies decreases with increasing *p* index and increasing temperature difference.
- The frequencies obtained for in the case of with point mass are always smaller than the frequency values obtained for in the case of without point mass.
- When the point mass is located on a nodal line, the mass does not move during these and so frequency remain constant as independent of the presence of mass. It is understood from this that if the mass is located on the nodal lines, at these frequencies it will resonate at the natural frequency of the unperturbed plate: e.g. for $a/b=1$, the second, the fourth and the sixth frequencies remain constant; for $a/b=1.5$ and 2, the second mode remains constant.
- When $a/b=1.5$ and 2, at high frequencies, intermediate frequencies occur in the case of with mass: e.g. it is seen that in the case of without mass the third and the fifth frequencies, respectively, equivalent in the case of with mass to the fourth and sixth frequencies.
- The *p* value and temperature are more effective at increasing *a*/*b* values in the case of with mass and accordingly the nodal lines are displaced.
- An increase in temperature always causes a decrease in the frequency value, regardless of the mass ratio and the position of the point mass, while this decrease becomes more temperature sensitive with increasing mass ratio.
- Increasing of the *p* value causes the frequency value to decrease regularly, in all mass ratio which considered and the location of the point mass.
- Temperature affects the vibration behavior in the form of the change of direction of the waves in some modes or the displacement of the mode shapes at some frequencies.
- The presence of point mass affects vibrational behavior in some modes by changing the direction of the waves or changing their mode shape or increasing the number of waves at some frequencies. In addition, in cases where the point mass is on the axis of symmetry, the vibration behavior occurs symmetrically with respect to the axis, while this symmetry is broken at points where the mass is outside the axis of symmetry.

Funding The author received no financial support for the research, authorship, and/or publication of this article.

Declarations

Conflict of interest The author declares that no conflicts of interest with respect to the research, authorship, and/or publication of this article.

References

1. Yamanouchi M, Koizumi M, Hirai T, Shiota I (1990) Proceedings of first international symposium on functionally graded materials. Sendai, Japan
2. Koizumi M (1993) The concept of FGM. Ceramic Transact Funct Graded Mater 34:3–10
3. Vu TV, Nguyen NH, Khosravifard A, Hematiyan MR, Tanaka S, Bui TQ (2017) A simple FSDT-based meshfree method for analysis of functionally graded plates. Eng Anal Boundary Elem 79:1–12
4. Zhao X, Lee YY, Liew KM (2009) Free vibration analysis of functionally graded plates using the element-free kp_Ritz method. J Sound Vib 319:918–939
5. Talha M, Singh BN (2010) Static response and free vibration analysis of FGM plates using higher order shear deformation theory. Appl Math Model 34:3991–4011
6. Nguyen TK (2015) A higher-order hyperbolic shear deformation plate model for analysis of functionally graded materials. Int J Mech Mater Design 11:203–219
7. Ferreira AJM, Batra RC, Roque CMC, Qian LF, Jorge RMN (2006) Natural frequencies of functionally graded plates by a meshless method. Compos Struct 75:593–600
8. Matsunaga H (2008) Free vibration and stability of functionally graded plates according to a 2-D higher-order deformation theory. Compos Struct 82:499–512
9. Dozio L (2014) Exact free vibration analysis of Lévy FGM plates with higher-order shear and normal deformation theories. Compos Struct 111:415–425
10. Jin G, Su Z, Shi S, Ye T, Gao S (2014) Three-dimensional exact solution for the free vibration of arbitrarily thick functionally graded rectangular plates with general boundary conditions. Compos Struct 108:565–577
11. Vel SS, Batra RC (2004) Three-dimensional exact solution for the vibration of functionallygraded rectangular plates. J Sound Vib 272:703–730
12. Mori T, Tanaka K (1973) Average stress in matrix and average elastic energyof materials with misfitting inclusions. Acta Metall 21:571–574
13. Benveniste Y (1987) A new approach to the application of Mori–Tanaka's theory of composite materials. Mech Mater 6:147–157
14. Hill R (1965) A self-consistent mechanics of composite materials. J Mech Phys Solids 13:213–222
15. Uymaz B, Aydoğdu M (2007) Three-dimensional vibration analyses of functionally graded plates under various boundary conditions. J Reinf Plast Compos 26:1847–1863
16. Natarajan S, Baiz PM, Ganapathi M, Kerfriden P, Bordas S (2011) Linear free flexural vibration of cracked functionally graded plates in thermal environment. Comput Struct 89(15–16):1535–1546
17. Kim YW (2005) Temperature dependent vibration analysis of functionally graded rectangular plates. J Sound Vib 284:531–549

18. Li Q, Iu VP, Kou KP (2009) Three-dimensional vibration analysis of functionally graded material plates in thermal environment. J Sound Vib 324:733–750
19. Gürgöze M, Özgür K, Erol H (1995) On the eigenfrequencies of a cantilevered beam with a tip mass and in-span support. Comput Struct 56(1):85–92
20. Cha PD, Wong WC (1999) A novel approach to determine the frequency equations of combined dynamical systems. J Sound Vib 219(4):689–706
21. Kopmaz O, Telli S (2002) Free vibrations of a rectangular plate carrying a distributed mass. J Sound Vib 251(1):39–57
22. Wong WO (2002) The effects of distributed mass loading on plate vibration behavior. J Sound Vib 252(3):577–583
23. Zhou D, Ji T (2006) Free vibration of rectangular plates with continuously distributed spring-mass. Int J Solids Struct 43:6502–6520
24. Alibeigloo A, Shakeri M, Kari MR (2008) Free vibration analysis of antisymmetric laminated rectangular plates with distributed patch mass using third-order shear eformation theory. Ocean Eng 35:183–190
25. Chiba M, Sugimoto T (2003) Vibration characteristics of a cantilever plate with attached spring–mass system. J Sound Vib 260:237–263
26. Yu SD (2009) Free and forced flexural vibration analysis of cantilever plates with attached point mass. J Sound Vib 321:270–285
27. Ciancio PM, Rossit CA, Laura PAA (2006) Approximate study of the free vibrations of a cantilever anisotropic plate carrying a concentrated mass. J Sound Vib 302(3):621–628
28. Aydoğdu M, Filiz S (2016) Vibration analysis of symmetric laminated composite plates with attached mass. Mech Adv Mater Struct 23(2):136–145
29. Watkins RJ, Santillan S, Radice J, Barton O Jr (2010) Vibration response of an elastically point-supported plate with attached masses. Thin-Walled Struct 48:519–527
30. Khalili SMR, Tafazoli S, Malekzadeh K, Mittal RK (2010) Geometrical effects of distributed attached mass on the natural frequency of thick cylindrical and spherical shells using higher-order theory. Turk J Eng Environ Sci 34:189–199
31. Maiz S, Rossit CA, Bambill DV, Susca A (2009) Transverse vibrations of a clamped elliptical plate carrying a concentrated mass at an arbitrary position. J Sound Vib 320:1146–1163
32. Zhou D, Cheung YK, Au FTK, Lo SH (2002) Three-dimensional vibration analysis of thick rectangular plates using Chebyshev polynomial and Ritz method. Int J Solids Struct 39(26):6339–6353
33. Gorman DJ (1976) Free vbiration analysis of cantilever plates by the method of superposition. J Sound Vib 49(4):453–467